Modeling subglacial sediment entrainment and the evolution of ice-sediment facies

Ethan Pierce[1, 2], Irina Overeem[1, 2]
1. Department of Geologic Sciences, University of Colorado Boulder, Boulder, CO, USA
2. Institute of Arctic and Alpine Research, Boulder, CO, USA

Background

- At glacial margins, we often see meters-thick layers of sediment entrained in ice near the base of the glacier (Figure 1, inset).
- Previous studies have attempted to link sedimentological properties with processes that may have entrained this debris in the subglacial environment [1-3].
- By doing so, we may be able to harness descriptions of sediment facies as a new archive for understanding the hydrology, thermodynamics, and topography beneath individual glaciers.
- It remains unclear, however, what mechanism(s) is (are) responsible for forming "dispersed" basal ice facies (e.g., Figure 2), especially given the prevalence of such layers across different regions, climate conditions, and glacial settings.
- Here, we use observations of basal ice facies from Mendenhall Glacier, AK, to inform the development of a numerical model to describe facies formation.
- In particular, our model describes the coevolution of debris-rich, stratified facies and debris-poor, dispersed facies beneath temperate glaciers.

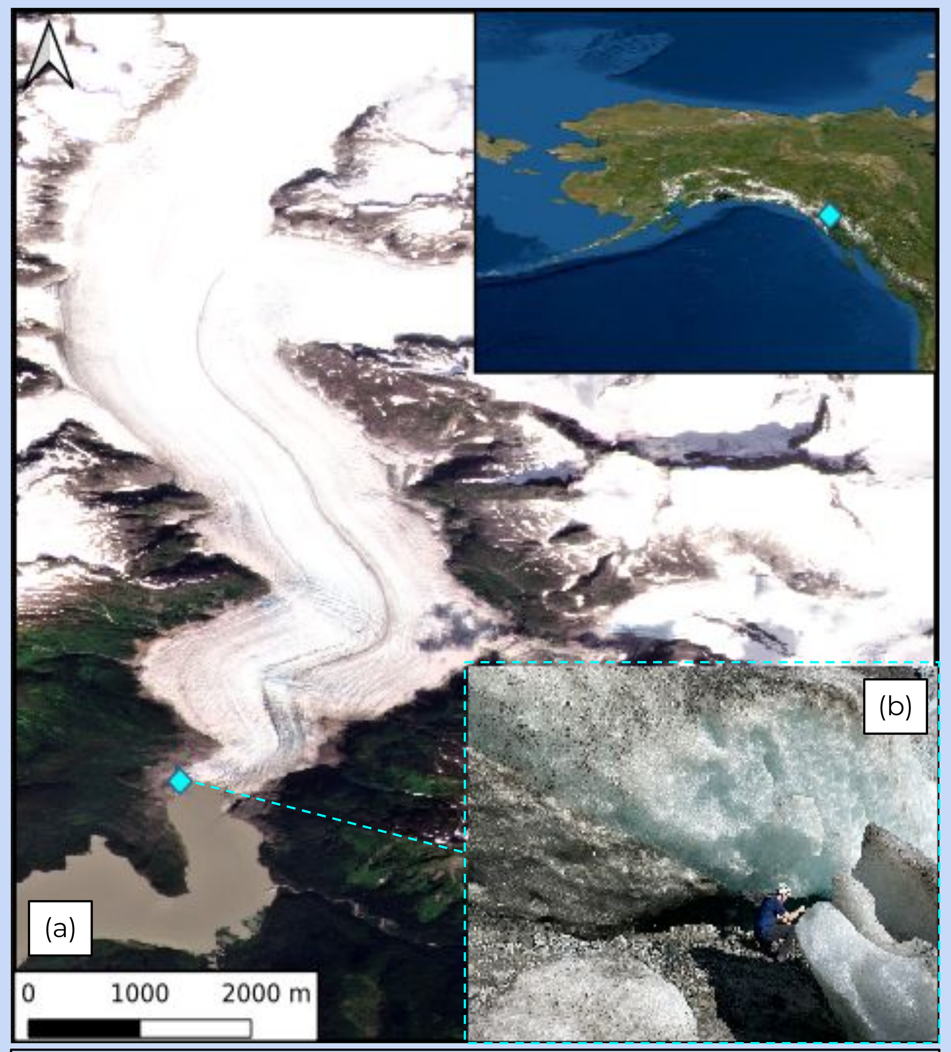

Figure 1. Observations of basal ice facies were collected at Mendenhall Glacier, Juneau, AK. The sampled margin is marked on map (a), along with a photograph of Column 1 (b).

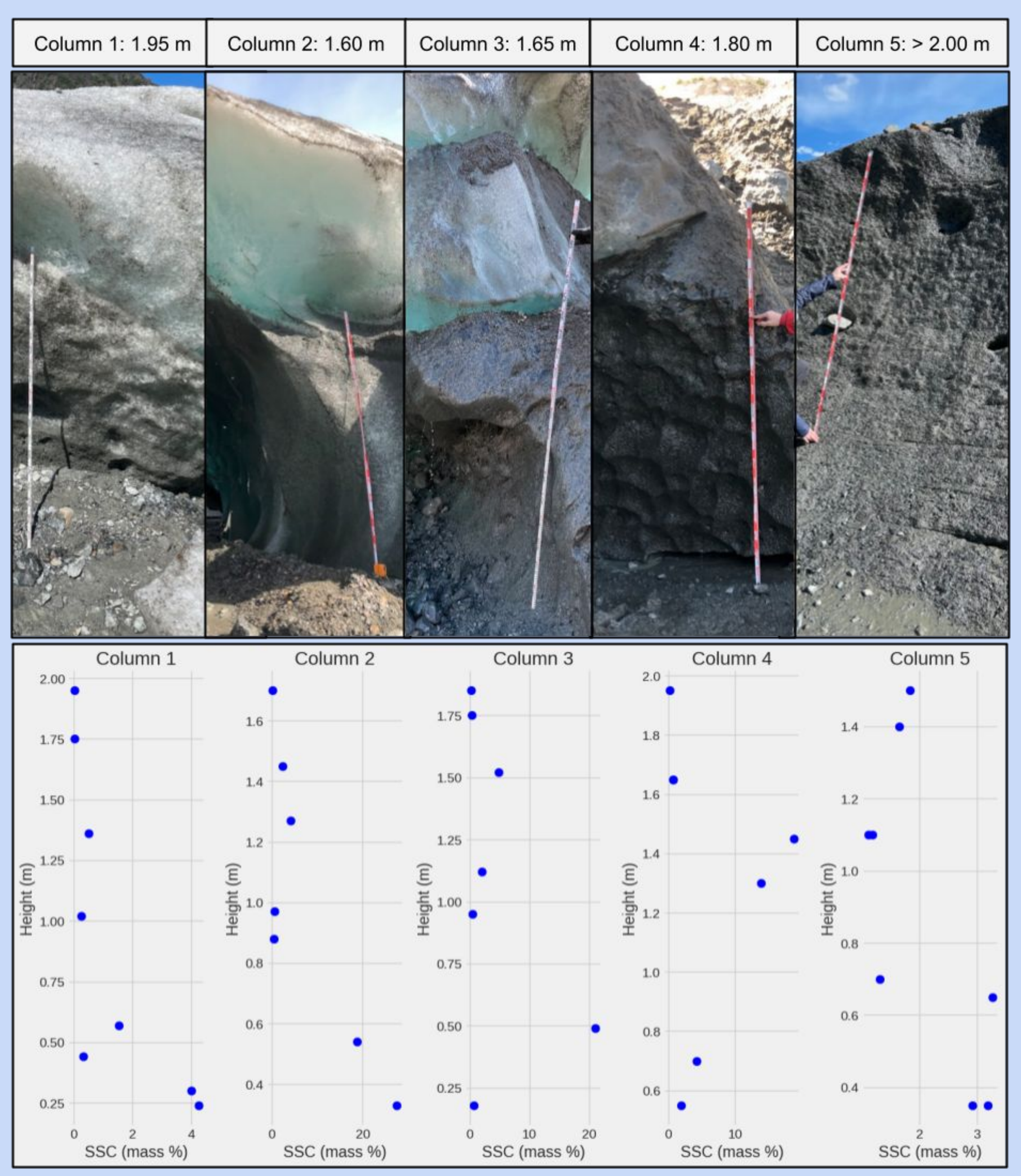

Figure 2. Photographs of each stratigraphic column (above), along with sediment concentrations (% mass) by height above the bed (below).

Observations

- At Mendenhall Glacier, we obtained sediment samples from 5 locations at the margin.
- Key measurements include overall layer thickness, measured in the field, and sediment concentration, measured by % mass.
- Qualitative observations were made on overall stratigraphic organization, the structure of each individual layer, the bubble content, clast size and spacing, angularity of clasts, and flocculation.
- This section of the margin is land-terminating, with ice flow moving from an overdeepening onto the terminal moraine. As such, the exposed layers all had a dip in the range of 24-32° to the NE.
- At each exposure, we took samples in duplicate columns, separated by ~1 m laterally. The maximum variation in sediment concentration from samples at the same depth was 3%.
- Five samples showed greater than 10% SSC, and only three of those samples were located above relatively debris-poor layers.
- Of the outlier samples, those around the 0.5-1 meter mark featured concentrated melting from redirected surface flow through rivulets and other micro-scale features.

Conceptual model

Given our observations at Mendenhall Glacier, we propose the following conceptual model for subglacial sediment entrainment (Figure 3):

1. At the ice-till interface (where basal slip occurs), a **frozen fringe** layer develops [4-5].
2. Between the frozen fringe and the englacial ice layer, **vertical regelation** drives the formation of a dispersed facies.
3. The layer nearest to the slip interface (usually frozen fringe) is thinned by basal melt.
4. Both layers are modulated by advective thickening or thinning, depending on the ice flow regime.

The following governing equations describe the constituent models and their coupled terms.

The height of the regelation layer, *Hr*, follows [6]:

$$\frac{\partial H_r}{\partial t} - \mathbf{u} \cdot \nabla H_r = K \frac{N}{H_f} - \frac{1}{\rho L} Qf \to r$$

where ***u*** is the sliding velocity, *K* is the array conductivity, *N* is the effective pressure, *ρ* is the ice density, *L* is the latent heat of fusion for ice, and *Qf→r* denotes the heat flux from the fringe.

The height of the fringe layer, *Hf*, follows [5]:

$$\frac{\partial H_f}{\partial t} + \mathbf{u} \cdot \nabla H_f = -\frac{\dot{m} + V}{\phi S}$$

where ***u*** is the sliding velocity, *m* is the basal melt rate at the ice-till interface, *V* is a combination of the heave force and pressure-induced entrainment, *Φ* is the till porosity, and *S* is the depth-averaged saturation of the substrate.

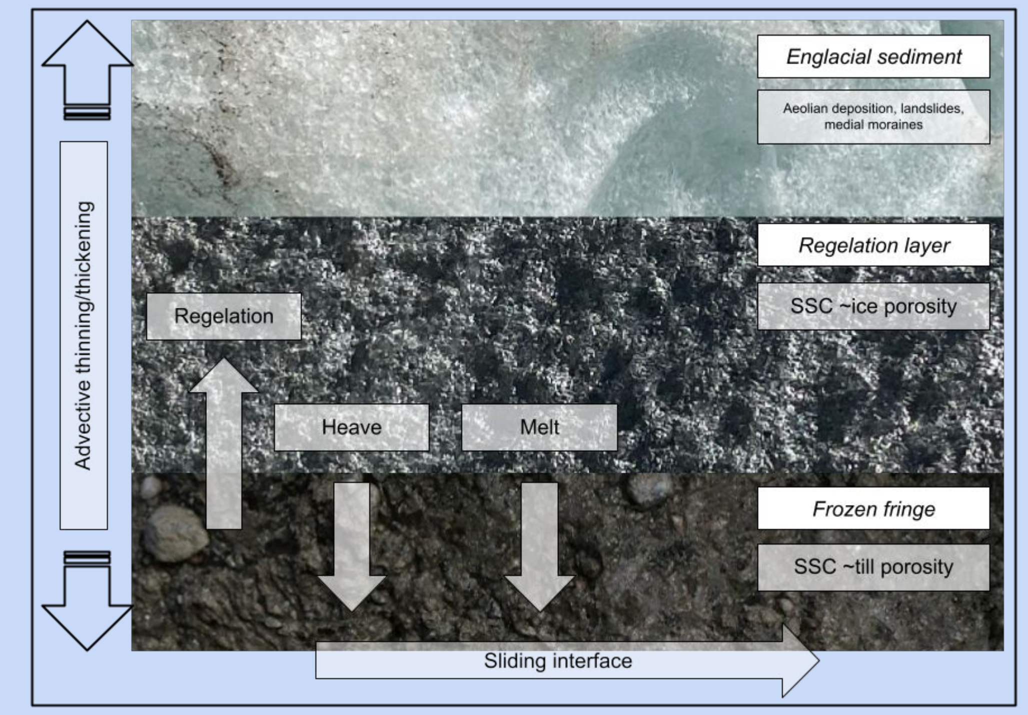

Figure 4. Overview of the conceptual model. The frozen fringe layer is set by a balance between effective pressure, frost heave, and basal melt. The regelation layer is set by the vertical motion of clasts from the top of the fringe into the englacial pore space.

Boundary conditions

- To implement the model depicted in Figure 4, we treat sliding velocity and effective pressure as diagnostic quantities.
- To estimate sliding velocity, we first obtained surface velocity from ITS_LIVE image pairs [7]. We then used a shallow ice approximation in *icepack* [8] to estimate the component of deformation. Sliding velocity is thus surface velocity – deformation velocity.
- We use two different estimates of effective pressure: for simulation (A), we assume a constant effective pressure of 100 kPa; for (B), we rescale overburden pressure by 10%, following the recommendation in [9].

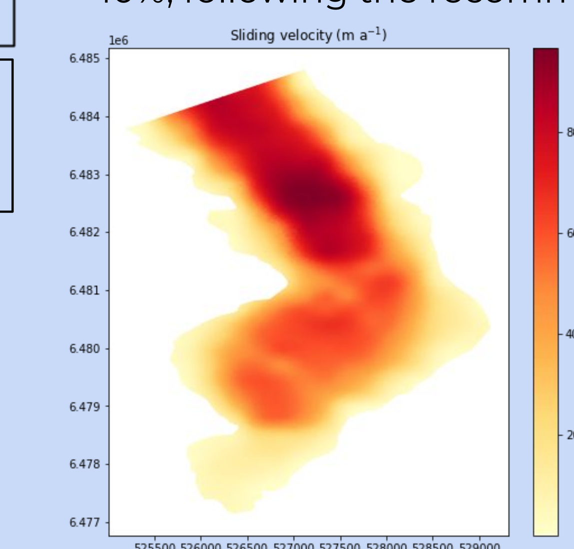

Figure 5. Estimated sliding velocity (from the flux gate) in meters per year.

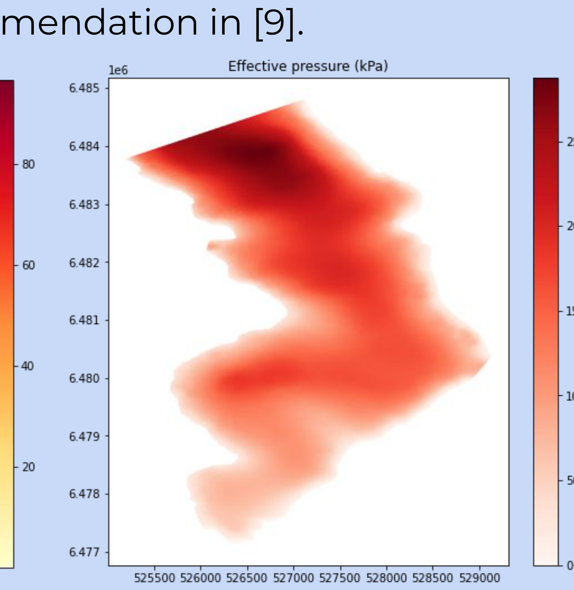

Figure 6. Scaled overburden pressure (from the flux gate) in kPa.

Results

- All model runs converged to a steady-state profile within a tolerance of 0.1 mm a^{-1} after 100 years or fewer.
- Figure 7 shows results from the regelation layer component. In both cases, the presence of frozen fringe insulates the regelation layer from basal melt. Spatial variations in layer thickness thus depend entirely on the effective pressure field.
- At the terminus, the regelation layer is 1.38 meters thick, with a porosity between 1% and 3%.
- Figure 8 shows results from the frozen fringe component. In contrast to the regelation layer, the fringe balances pressure-induced entrainment with basal melt, and as such shows less spatial variability in the scenario where effective pressure is not constant.
- At the terminus, the fringe layer is 1.66 meters thick, with a till porosity around 35%.

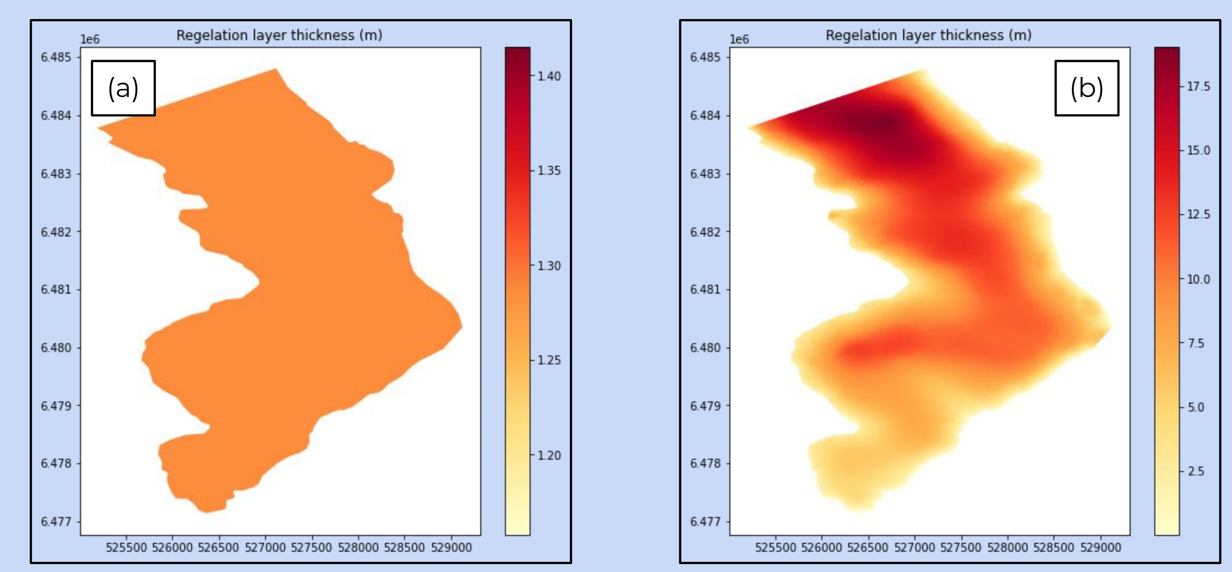

Figure 7. Predicted steady-state thickness of the regelation layer, with a constant effective pressure of 100 kPa (a), or a variable effective pressure depending on overburden (b).

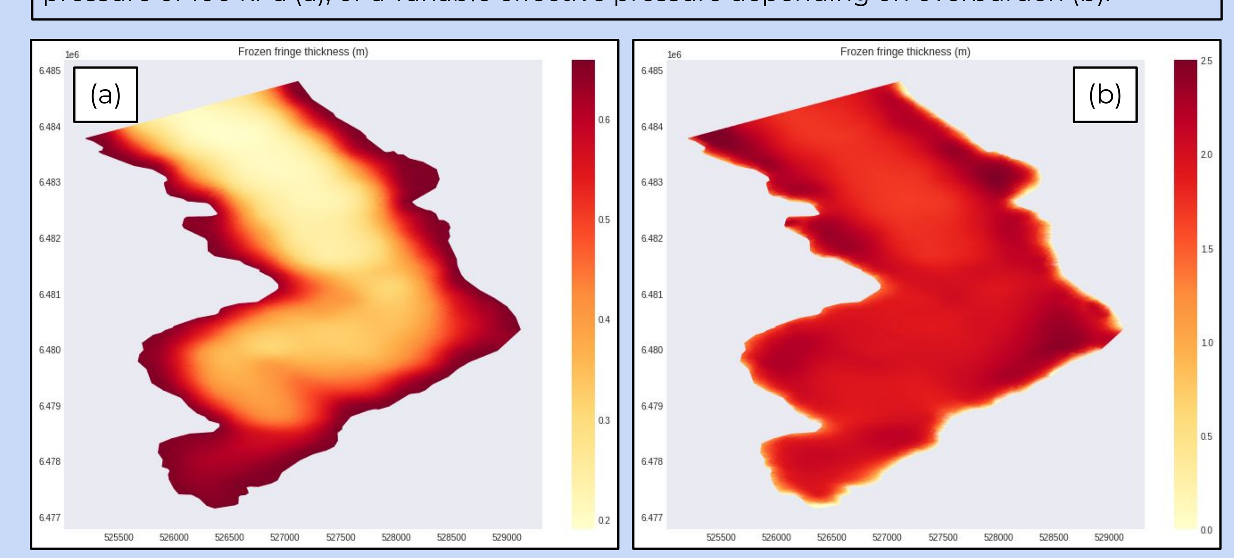

Figure 8. Predicted steady-state thickness of the fringe layer, with a constant effective pressure of 100 kPa (a), or a variable effective pressure depending on overburden (b).

Interpretation

Based on our model results and previously published information on regelation and fringe mechanics, we are able to reconstruct the predicted sediment column at the terminus (Figure 9). Our model predicts a 1.66 m stratified facies at the bed, driven by frozen fringe evolution, and featuring high sediment concentrations. Above that lies a 1.38 m dispersed facies, driven by vertical regelation, featuring decreasing sediment concentrations with height.

This interpretation relies on the key assumption that SSC in the fringe is driven by till porosity, while in the regelation layer it is governed by ice porosity. This distinction stems from defining the fringe as a thermal boundary layer in the substrate, and the regelation layer as a diffusive contact in the basal ice structure.

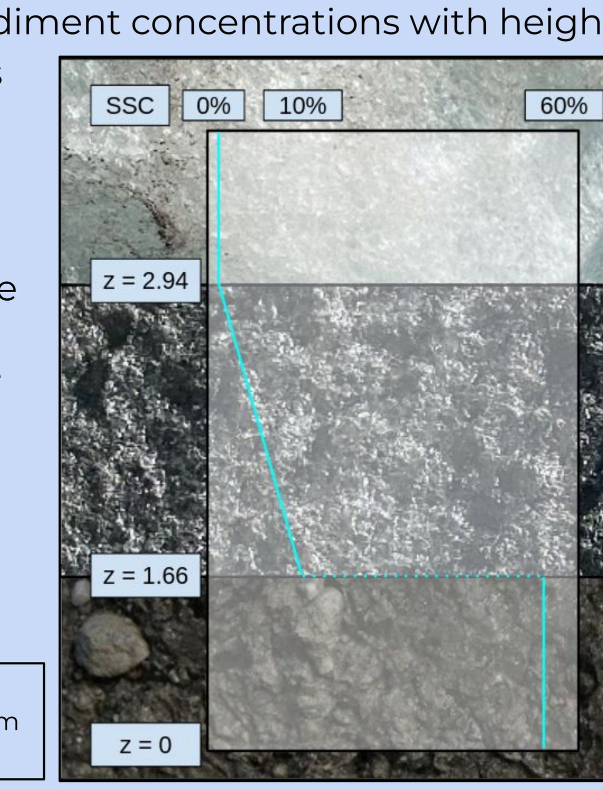

Figure 9. Predicted ice stratigraphy, given the results from the (scaled-N) numerical model.

Modeling targets

From the observations shown in Figure 2, we identify a continuous "dispersed" ice facies across Mendenhall's margin. The characteristic features of this layer are:

- Massive structure on meter-scales
- Between 1.5 and 2 meters thick
- Low sediment concentrations (1 - 10% by mass)
- Angular clasts
- Polymodal size distribution (sand - pebbles - cobbles)
- Low bubble concentrations (1 - 10 cm spacing)
- Sediment emplaced within the ice matrix

Additionally, we have *limited* evidence for the presence of a "stratified" layer beneath the dispersed facies. The characteristic features of this layer are:

- Stratification on centimeter- to decimeter-scales
- Diffuse contact with the dispersed facies above
- Higher sediment concentrations (>> 20% by mass)
- Angular clasts
- Polymodal size distribution, with many large clasts
- Located above the slip interface, based on dip angle
- Interstitial ice incorporated into the underlying till

Future work

- Currently, both effective pressure and ice porosity are unconstrained parameters. For the regelation layer in particular, these variables are first-order controls on the total volume of entrained sediment.
- To further constrain the dispersed facies model, we are in the process of adapting an englacial enthalpy model from [10]. This will solve for ice porosity, the pore-pressure gradient between the regelation layer and fringe layer, and basal melting or refreezing, independent of either facies model.
- Further steps include review prior hypotheses for dispersed facies formation, and attempting to reproduce field observations using the models described here.
- By modeling the entrainment of sediment in glacial ice, we will refine estimates of how sediment transport is partitioned in glacial catchments and predict how subglacial sedimentary systems may respond to future changes in climate.

References and acknowledgements

1. Lawson, D. E. (1979). Sedimentological analysis of the western terminus region of the Matanuska Glacier, Alaska.
2. Hubbard, B., Cook, S., & Coulson, H. (2009). Basal ice facies: a review and unifying approach. Quaternary Science Reviews, 28(19-20), 1956-1969.
3. Cook, S. J., Swift, D. A., Graham, D. J., & Midgley, N. G. (2011). Origin and significance of 'dispersed facies' basal ice: Svínafellsjökull, Iceland. Journal of Glaciology, 57(204), 710-720.
4. Rempel, A. W. (2008). A theory for ice-till interactions and sediment entrainment beneath glaciers. Journal of Geophysical Research: Earth Surface, 113(F1).
5. Meyer, C. R., Robel, A. A., & Rempel, A. W. (2019). Frozen fringe explains sediment freeze-on during Heinrich events. Earth and Planetary Science Letters, 524, 115725.
6. Iverson, N. R., & Semmens, D. J. (1995). Intrusion of ice into porous media by regelation: A mechanism of sediment entrainment by glaciers. Journal of Geophysical Research: Solid Earth, 100(B6), 10219-10230.
7. Gardner, A. S., M. A. Fahnestock, and T. A. Scambos, 2019. MEaSUREs ITS_LIVE Landsat Image-Pair Glacier and Ice Sheet Surface Velocities: Version 1.
8. Shapero, D. R., Badgeley, J. A., Hoffman, A. O., & Joughin, I. R. (2021). icepack: A new glacier flow modeling package in Python, version 1.0. Geoscientific Model Development, 14(7), 4593-4616.
9. Flowers, G. E. (2015). Modelling water flow under glaciers and ice sheets. Proceedings of the Royal Society A: Mathematical, Physical and Engineering Sciences, 471(2176), 20140907.
10. Hewitt, I. J., & Schoof, C. (2017). Models for polythermal ice sheets and glaciers. The Cryosphere, 11(1), 541-551.

Field data collection was funded by a CU Boulder Innovation Seed Grant. Model development efforts were funded by NSF award 2104102. Laboratory analyses were supported by SEEL shared lab space and the expertise of W. Roth. We would also like to acknowledge B. Carlson, A. Moodie, and A. Eckland for their assistance in the field.